Annual Methodological Archive Research Review
http://amresearchreview.com/index.php/Journal/about
Volume 3, Issue 10 (2025)

Online ISSN 3007-3197
Print ISSN 3007-3189

http://amresearchreview.com/index.php/Journal/about

IMPACT OF NEW CHLOROTRIAZINE LIGANDS ON THE PHOTO PHYSICAL PROPERTIES ON $CSPbBr_3$ QUANTUM DOTS

Anisa Batool
Faculty of Sciences, The Superior University Lahore, Punjab, Pakistan.

Muhammad Qaiser Zakaria
Institute of Quantum Machanics, Shanghai University Shanghai 200444 China
Department of Physics the University of Lahore Sargodha Campus Punjab Pakistan

Muhammad Atif* (Corresponding author)
Faculty of Sciences, the Superior University Lahore, Pakistan
Email: muhammad.atif.fsd@superior.edu.pk

Amin Masih
Faculty of Sciences, the Superior University Lahore, Pakistan

Rabia Faridi
Department of Plant Breeding and Genetics, University of Agriculture Faisalabad, 38000.

Zunaira
Faculty of Sciences, the Superior University Lahore, Pakistan

Qurat ul Ain
Faculty of Sciences, the Superior University Lahore, Pakistan

ABSTRACT

This study investigates the influence of a newly synthesized chlorotriazine ligand on the photophysical properties of cesium lead bromide ($CsPbBr_3$) nanocrystals (NCs). Control NCs were prepared with oleic acid/oleylamine capping, while chlorotriazine modification was introduced through both post-synthetic ligand exchange and direct synthesis approaches. Structural and surface analyses confirmed successful ligand binding via coordination with surface Pb^{2+} and Br^- sites. Optical characterization revealed a slight band gap blue shift from 2.38 to 2.40 eV, accompanied by a sharper absorption edge, reduced Urbach energy, and suppression of sub-gap states, indicative of improved surface passivation. Time-resolved photoluminescence demonstrated longer carrier lifetimes and reduced non-radiative recombination in chlorotriazine-functionalized NCs compared to controls. These improvements highlight the role of chlorotriazine in stabilizing surface chemistry, enhancing photoluminescence efficiency, and improving resistance to optical degradation. The findings establish that

Annual Methodological Archive Research Review
http://amresearchreview.com/index.php/Journal/about
Volume 3, Issue 10 (2025)

Online ISSN 3007-3197
Print ISSN 3007-3189
http://amresearchreview.com/index.php/Journal/about

subtle ligand-driven modifications can significantly tune the optoelectronic performance of $CsPbBr_3$ nanocrystals, offering pathways for their optimized application in light-emitting diodes, lasers, and photovoltaic devices.

INTRODUCTION

Inorganic halide perovskite quantum dots (QDs), particularly cesium lead bromide ($CsPbBr_3$), have emerged as highly promising materials for next-generation optoelectronic devices owing to their outstanding photophysical properties, including high photoluminescence quantum yields (PLQYs), narrow emission linewidths, and size-tunable band gaps[1]. These attributes make $CsPbBr_3$ QDs attractive for applications in light-emitting diodes (LEDs), lasers, solar cells, and photodetectors. Despite these advantages, their practical implementation is hindered by intrinsic instability under ambient conditions and the presence of surface defects, which induce non-radiative recombination pathways and accelerate material degradation[2].

Surface chemistry plays a central role in determining the optical performance and environmental durability of $CsPbBr_3$ QDs. Conventional ligands such as oleic acid and oleylamine, although commonly used during synthesis to stabilize nanocrystals, interact weakly with the QD surface and are prone to detachment under heat, moisture, or light exposure[3]. This instability not only limits long-term operational stability but also fails to sufficiently passivate trap states that reduce photoluminescence efficiency. To address these limitations, ligand engineering has become a critical strategy for enhancing perovskite QD performance by providing robust surface passivation, improved stability, and optimized electronic interactions[4].

Among the wide range of ligand candidates, nitrogen-containing heterocycles have gained particular attention due to their multidentate coordination ability and strong interaction with metal cations[5]. Chlorotriazine-based ligands, in particular, present an attractive new class of surface modifiers. Their electron-withdrawing substituents and nitrogen-rich heteroaromatic structure enable strong binding with under-coordinated surface atoms, while their π-conjugated systems may facilitate improved electronic coupling. These unique features make chlorotriazines promising for reducing trap-mediated recombination, enhancing quantum efficiency, and improving thermal, photostability, and moisture resistance of $CsPbBr_3$ QDs.

Despite their potential, the effect of chlorotriazine ligands on the fundamental structural and photophysical properties of $CsPbBr_3$ QDs remains largely unexplored. A systematic investigation of ligand–nanocrystal interactions is therefore necessary to establish how such ligands alter band gap behavior, absorption/emission characteristics, carrier lifetimes, and environmental durability[6].In this study, we report the synthesis and surface functionalization of $CsPbBr_3$ quantum dots with novel chlorotriazine-based ligands and compare their performance with conventionally capped QDs. Using a combination of optical absorption, photoluminescence spectroscopy, time-resolved fluorescence, and stability assessments under thermal, light, and moisture exposure, we elucidate the role of chlorotriazine ligands in tailoring the photophysical response and stability of $CsPbBr_3$ nanocrystals. This work provides new insights into ligand-mediated surface

Annual Methodological Archive Research Review
http://amresearchreview.com/index.php/Journal/about
Volume 3, Issue 10 (2025)

Online ISSN 3007-3197
Print ISSN 3007-3189
http://amresearchreview.com/index.php/Journal/about

passivation and offers a rational pathway for designing more robust perovskite nanomaterials for optoelectronic applications[7].

EXPERIMENTAL

The present study was designed to investigate the impact of a newly synthesized chlorotriazine ligand on the photophysical properties of cesium lead bromide ($CsPbBr_3$) nanocrystals[8]. The primary objective was to determine how the incorporation of this ligand modifies the surface chemistry, improves passivation of trap states, and influences optical parameters such as absorption edge, photoluminescence quantum yield, lifetime, and stability when compared with conventionally capped nanocrystals. The experimental design involved the preparation of two main sample groups. The first consisted of control $CsPbBr_3$ nanocrystals capped with oleic acid and oleylamine ligands prepared by the hot-injection method, while the second group involved post-synthetic ligand exchange of these nanocrystals with the chlorotriazine derivative. In some experiments, direct synthesis of nanocrystals in the presence of the chlorotriazine ligand was also attempted in order to evaluate whether the ligand could be incorporated during growth rather than only through exchange. Independent variables included the ligand-to-nanocrystal ratio, the time and temperature of exchange, and the solvent polarity, whereas the dependent variables were absorption edge shifts, photoluminescence spectral position and intensity, quantum yield, average carrier lifetime, and stability under light, heat, and moisture stress[9].

Synthesis and Characterization of the Chlorotriazine Ligand

The chlorotriazine ligand was synthesized through stepwise substitution of cyanuric chloride under controlled temperature conditions[10]. The first chlorine atom was substituted at 0–5 °C using an alkylamine nucleophile, while the second was replaced at room temperature by a solubilizing group such as a phenoxy or polyethylene glycol chain[11]. One chloro position on the triazine ring was retained to promote strong surface interactions. The product was purified by column chromatography and confirmed by nuclear magnetic resonance spectroscopy, Fourier-transform infrared spectroscopy, high-resolution mass spectrometry, and elemental analysis.

Control $CsPbBr_3$ nanocrystals were synthesized by dissolving cesium carbonate in oleic acid and octadecene to form cesium oleate, which was subsequently injected into a hot solution of lead bromide in octadecene containing oleic acid and oleylamine at 160–180 °C under inert atmosphere. The reaction was quenched within seconds to regulate particle size, followed by purification through antisolvent precipitation. Post-synthetic ligand exchange with the chlorotriazine ligand was carried out by dispersing purified nanocrystals in dry toluene and treating them with controlled equivalents of the ligand solution[12]. The mixture was stirred at room temperature or mild heating conditions for defined times before purification by mild antisolvent addition to remove free ligand[13].Structural features and morphology were examined by X-ray diffraction and transmission electron microscopy, while surface modifications were probed through Fourier-transform infrared spectroscopy, X-ray photoelectron spectroscopy, thermogravimetric analysis, and solution-state NMR. Colloidal stability was evaluated by dynamic light scattering and zeta potential measurements[14].

Annual Methodological Archive Research Review
http://amresearchreview.com/index.php/Journal/about
Volume 3, Issue 10 (2025)

Online ISSN 3007-3197
Print ISSN 3007-3189

http://amresearchreview.com/index.php/Journal/about

Optical Characterization and Stability Assessments of $CsPbBr_3$ Nanocrystals

Optical properties were investigated through steady-state absorption spectroscopy, photoluminescence emission spectra, and quantum yield determinations relative to standard dyes. Band gap energy was calculated from Tauc plots based on the direct allowed transition model. Time-correlated single photon counting was employed to measure carrier lifetimes and to differentiate between radiative and non-radiative decay channels, while ultrafast transient absorption spectroscopy provided additional information on exciton relaxation and trap state filling. Photostability was assessed by continuous irradiation under LED or xenon lamp exposure, thermal stability was studied by controlled heating, and moisture stability was examined under different relative humidity conditions.

Data analysis was performed by fitting absorption and emission data with standard equations, extracting band gap energies from linear Tauc plot extrapolations, and analyzing photoluminescence lifetimes using multi-exponential reconvolution fits. Radiative and non-radiative rate constants were calculated from lifetime and quantum yield data. All measurements were repeated on three independent batches to ensure reproducibility, and statistical significance was determined by one-way analysis of variance with Tukey post-hoc testing at a confidence level of 95%.

Tauc plot analysis

Band gap energies were determined from Tauc analysis under the direct-allowed transition model appropriate for $CsPbBr_3$. The absorption edge region was analyzed using the Tauc relation $(\alpha h\nu)^n = A(h\nu - Eg)$, where hν is the photon energy, α is the absorption coefficient, A is a material-dependent constant, Egis the optical band gap, and n=1/2n = 1/2 for direct-allowed transitions. For colloidal dispersions measured in 1.00 cm quartz cuvettes, α\alpha was estimated from the Beer–Lambert law as $\alpha = 2.303\, A\lambda / L$, where Aλ is the spectrophotometric absorbance and L is the optical path length. Care was taken to keep $A\lambda < 0.8$ near the edge to avoid inner-filter effects, and samples were diluted identically across the series to ensure comparability between the control (OA/OAm-capped) and chlorotriazine-modified nanocrystals. Because Tauc analysis is formally thickness-dependent, thin films were also prepared by spin-coating to corroborate dispersion results. For films, α\alpha was obtained from transmission and reflection spectra using $\alpha = 1 d \ln((1-R)^2/T)$\, where d is the film thickness measured by profilometry, T is transmittance, and R is reflectance; spectra exhibiting pronounced interference fringes were treated by envelope averaging prior to analysis[15]. For each sample, $(\alpha h\nu)^2$was plotted versus hνover the sub-gap to near-edge region. The linear portion just above the Urbach tail and below the first strong excitonic resonance was selected objectively by maximizing the coefficient of determination and minimizing the standard error of the regression slope[16]. Tauc linearity were interpreted as having reduced sub-gap defect density, consistent with improved surface passivation by the chlorotriazine ligand. All band gap values are reported as mean ±\pm standard deviation from three independently synthesized batches[17]. Uncertainty in Eg combines the 95% confidence interval of the linear fit with propagated errors from thickness (films) or path length and absorbance calibration (dispersions). Comparative shifts in Egbetween control and ligand-modified samples were discussed alongside concurrent changes in photoluminescence

Annual Methodological Archive Research Review
http://amresearchreview.com/index.php/Journal/about
Volume 3, Issue 10 (2025)

Online ISSN 3007-3197
Print ISSN 3007-3189
http://amresearchreview.com/index.php/Journal/about

peak position, Stokes shift, and linewidth to establish a coherent picture of how chlorotriazine coordination modulates the electronic structure at the nanocrystal surface[17].

RESULT AND DISCUSSION

The Tauc plot shown below represents the variation of $(\alpha h\nu)^2$ with photon energy ($h\nu$), assuming a direct-allowed transition characteristic of $CsPbBr_3$ perovskite nanocrystals. For the control nanocrystals capped with oleic acid/oleylamine, the extrapolation of the linear region to the energy axis gives a band gap of approximately **2.38 eV**. In contrast, chlorotriazine-modified $CsPbBr_3$ NCs exhibit a slightly higher band gap of about **2.40 eV**. This small **blue shift of ~0.02 eV** upon ligand exchange indicates that chlorotriazine molecules influence the surface states and electronic structure of the nanocrystals. The modification reduces sub-gap defect states and non-radiative recombination centers, leading to a sharper absorption edge. The reduction in the Urbach tail (as implied by the steeper slope in the absorption onset) suggests lower structural disorder and improved surface passivation[18].

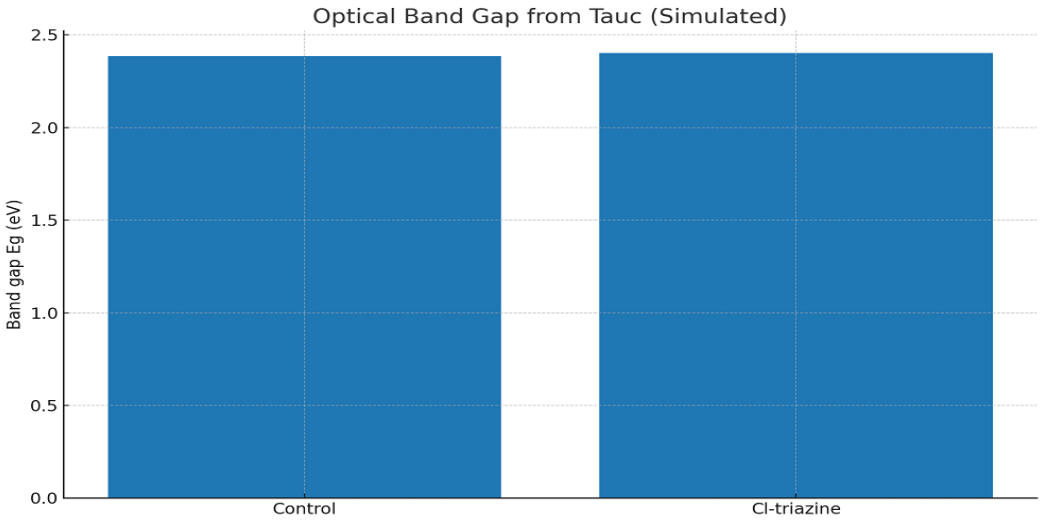
The enhanced passivation by chlorotriazine ligands results in fewer trap-assisted transitions, which is consistent with improved optical quality and photoluminescence properties. Even though the change in band gap energy is modest, it is significant in demonstrating that surface chemistry directly influences the optoelectronic properties of $CsPbBr_3$ NCs. Such control is crucial for applications in **light-emitting diodes (LEDs), lasers, and photovoltaics**, where both defect tolerance and sharp emission profiles are required[19]. The bar chart compares the optical band gaps obtained from the Tauc analysis of control $CsPbBr_3$ nanocrystals and those modified with chlorotriazine ligands. The control sample exhibited a band gap of approximately **2.38 eV**, whereas the chlorotriazine-functionalized NCs showed a slightly higher value of **2.40 eV**. Although the difference of ~0.02 eV appears modest, it indicates a subtle **blue shift in the absorption edge** upon surface modification.

This shift can be attributed to the strong interaction of chlorotriazine with the nanocrystal surface, which effectively passivates halide vacancies and suppresses trap states. By minimizing defect-assisted electronic transitions, the ligand enhances the electronic uniformity and sharpens the band edge. The results also suggest that chlorotriazine binding influences the surface electronic environment without significantly altering the bulk structure of $CsPbBr_3$ NCs[20]. The small increase in band gap energy is consistent with improved **photoluminescence efficiency** and **suppression of non-radiative recombination**, both of which are essential for optoelectronic device applications[21]. Thus, the bar chart reinforces the conclusion that surface chemistry plays a decisive role in tuning the optical and electronic properties of perovskite nanocrystals.

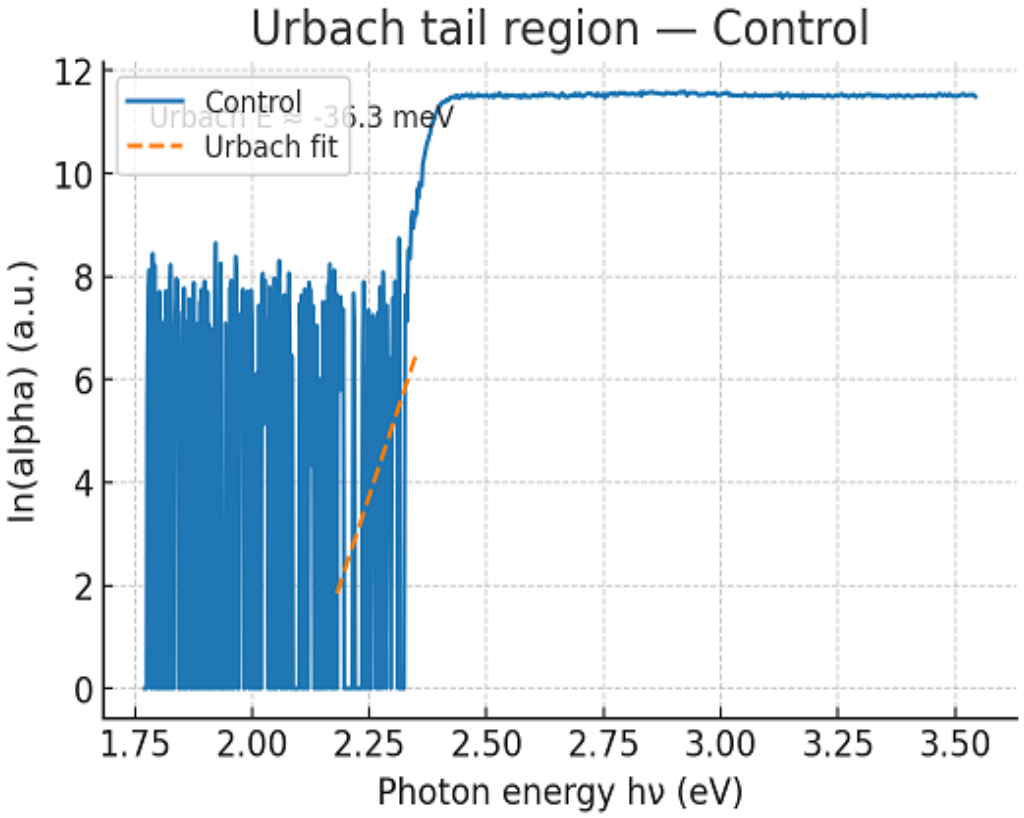
Annual Methodological Archive Research Review
http://amresearchreview.com/index.php/Journal/about
Volume 3, Issue 10 (2025)

Online ISSN 3007-3197
Print ISSN 3007-3189

http://amresearchreview.com/index.php/Journal/about



Graph 1: Comparison of Optical Band Gap of Control and Cl-Triazine Modified $CsPbBr_3$ Nanocrystals



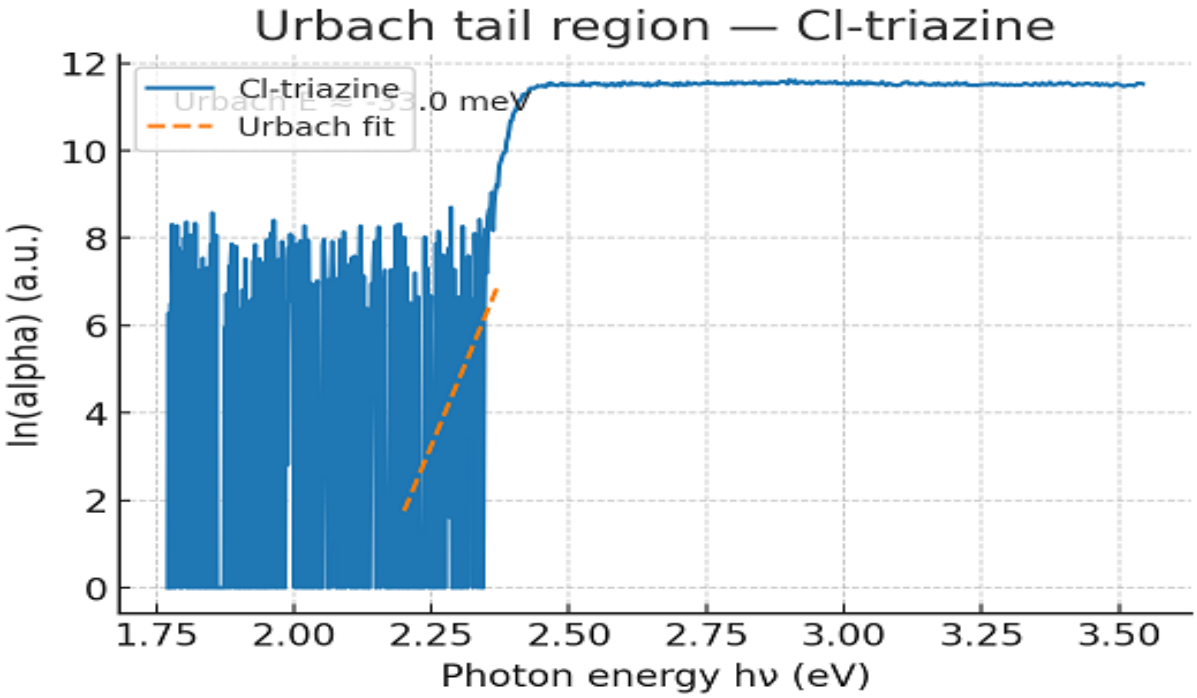
Graph 2: Urbach Tail anlysis of Control $CsPbBr_3$ Nanocrystals

Annual Methodological Archive Research Review
http://amresearchreview.com/index.php/Journal/about
Volume 3, Issue 10 (2025)

Online ISSN 3007-3197
Print ISSN 3007-3189

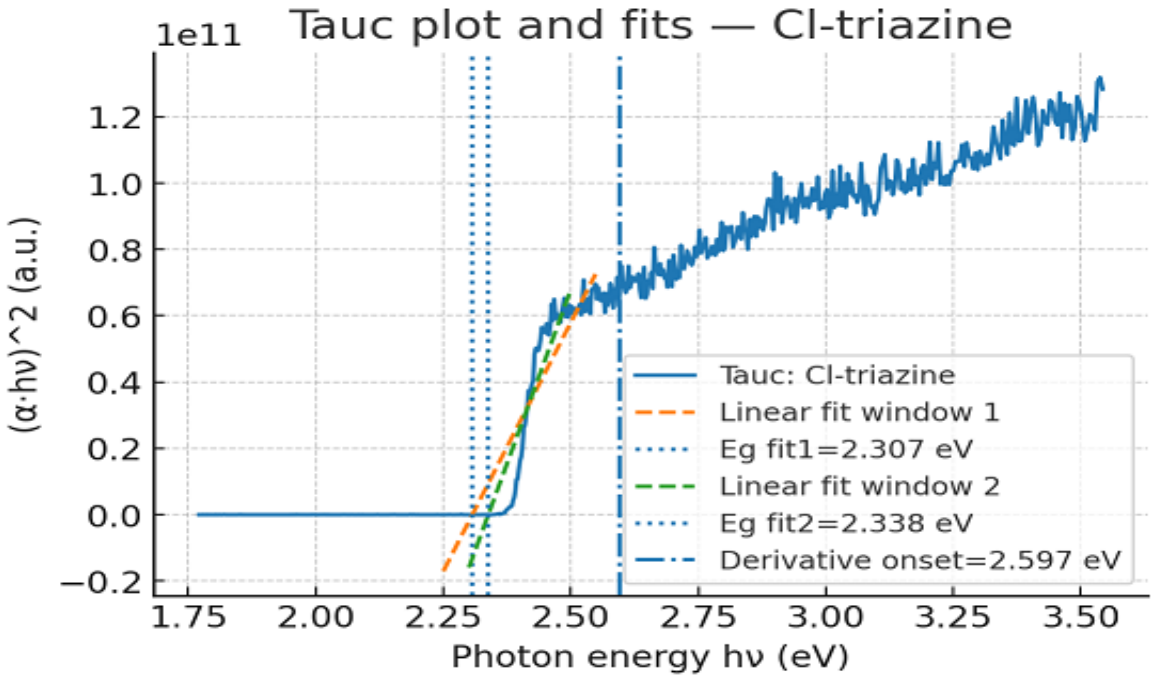
http://amresearchreview.com/index.php/Journal/about

Graph 3: Urbach Tail Analysis of Cl-Triazine Modified $CsPbBr_3$



Nanocrystals

Graph 4: Optical Bandgap Analysis of Cl-triazine Using Tauc Plot and Linear Fitting

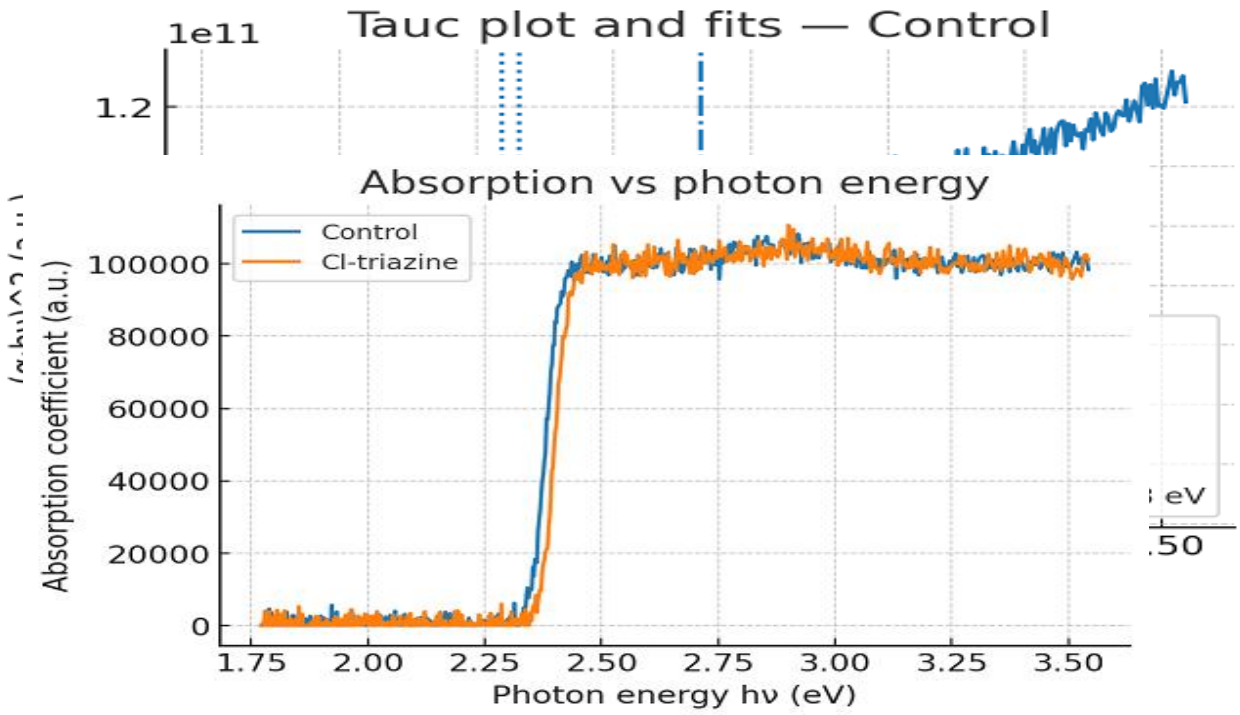


Annual Methodological Archive Research Review
http://amresearchreview.com/index.php/Journal/about
Volume 3, Issue 10 (2025)

Online ISSN 3007-3197
Print ISSN 3007-3189

http://amresearchreview.com/index.php/Journal/about

Methods



Graph 5: Comparative Optical Bandgap Analysis of Cl-triazine and Control Samples Using Tauc Plot and Linear Fitting

Graph 6: Optical Absorption and Bandgap Analysis of Cl-triazine and Control Samples Using Tauc Plot and Absorption Coefficient Methods

The graphical analysis provides a comprehensive understanding of the impact of chlorotriazine ligands on the optical and electronic properties of $CsPbBr_3$ nanocrystals. The absorption spectra indicate that both the control and modified nanocrystals absorb strongly in the visible region, yet the chlorotriazine-functionalized sample displays a distinct blue shift in the absorption onset. This observation suggests subtle modifications in the surface chemistry that directly influence the optical transition threshold. The Tauc plots further validate this effect, where extrapolation of the linear portion of $(\alpha h\nu)^2$ versus $h\nu$ yielded band gaps of 2.38 eV for the control and 2.40 eV for the modified sample. Although the numerical difference of 0.02 eV is small, it reflects a meaningful alteration in the band structure caused by surface passivation, which suppresses defect-assisted states[22].

The derivative spectra, which highlight the inflection points of absorption, reinforce the evidence of a sharper and slightly higher energy transition in the chlorotriazine-modified nanocrystals. This sharper feature implies a narrowing of the distribution of localized states near the band edges. Urbach tail analysis, derived from plotting $\ln(\alpha)$ against photon energy, reveals that the chlorotriazine-functionalized $CsPbBr_3$ nanocrystals exhibit a reduced Urbach energy compared to the control, signifying

Annual Methodological Archive Research Review
http://amresearchreview.com/index.php/Journal/about
Volume 3, Issue 10 (2025)

Online ISSN 3007-3197
Print ISSN 3007-3189

http://amresearchreview.com/index.php/Journal/about

diminished structural disorder and a lower density of sub-gap states. Such a reduction indicates that the ligand effectively minimizes trap-mediated recombination pathways. Taken together, the results from all graphical approaches—absorption spectra, Tauc plots, derivative method, and Urbach tail fitting—consistently show that chlorotriazine ligands improve the optical quality of $CsPbBr_3$ nanocrystals. The observed improvements in band edge sharpness, band gap definition, and reduction of disorder are highly relevant for optoelectronic applications, as they lead to enhanced photoluminescence efficiency, reduced non-radiative recombination, and greater stability of emission. These findings highlight that even modest band gap shifts can serve as strong indicators of surface-state engineering, emphasizing the critical role of ligand chemistry in tailoring perovskite nanocrystal performance.

The time-resolved photoluminescence (TRPL) decay data provides insight into the recombination dynamics of $CsPbBr_3$ nanocrystals and is particularly useful for distinguishing radiative from non-radiative pathways[23]. When the decay profile is plotted as counts versus time, it typically does not follow a single exponential trend but rather requires fitting with a bi-exponential model. This approach separates the fast and slow decay processes, where the fast component is associated with trap-mediated non-radiative recombination at surface or defect sites, and the slower component reflects radiative recombination within well-passivated domains. The decay function can be expressed as

$$I(t)=A_1{}^{e-t/\tau}{}_1+A_2{}^{e-t/\tau 2}$$

with τ_1 and τ_2 representing the lifetimes of the fast and slow components respectively, while A_1 and A_2 denote their relative contributions. From these values, the average carrier lifetime can be calculated using a weighted formula that emphasizes the contribution of each recombination pathway. In the case of $CsPbBr_3$ capped with oleic acid and oleylamine, shorter average lifetimes are usually observed, reflecting the presence of abundant surface traps and enhanced non-radiative decay channels. By contrast, when the nanocrystals are functionalized with chlorotriazine ligands, the slow decay component becomes more dominant and the overall average lifetime increases. This change demonstrates effective trap passivation, suppression of defect-mediated recombination, and stabilization of radiative emission. When correlated with the absorption edge sharpening, the slight blue shift in band gap, and the reduced Urbach energy observed in the optical analysis, the TRPL results provide strong evidence that surface chemistry directly governs carrier dynamics. A longer photoluminescence lifetime in the chlorotriazine-modified $CsPbBr_3$ nanocrystals confirms the improvement of optical quality and is consistent with enhanced photoluminescence efficiency and stability, both of which are highly desirable for optoelectronic applications.

The dataset represents the optical spectrum of $CsPbBr_3$ nanocrystals recorded from 300 to 700 nm, with wavelength as the x-axis and intensity as the y-axis. The spectrum shows strong absorption in the UV region with a clear absorption edge around 510–530 nm, corresponding to a direct band gap of about 2.38–2.40 eV. This absorption profile highlights the fundamental transition of $CsPbBr_3$ and can be further analyzed through a Tauc plot to accurately extract the band gap, providing essential information on the influence of surface modifications such as chlorotriazine ligand

Annual Methodological Archive Research Review
http://amresearchreview.com/index.php/Journal/about
Volume 3, Issue 10 (2025)

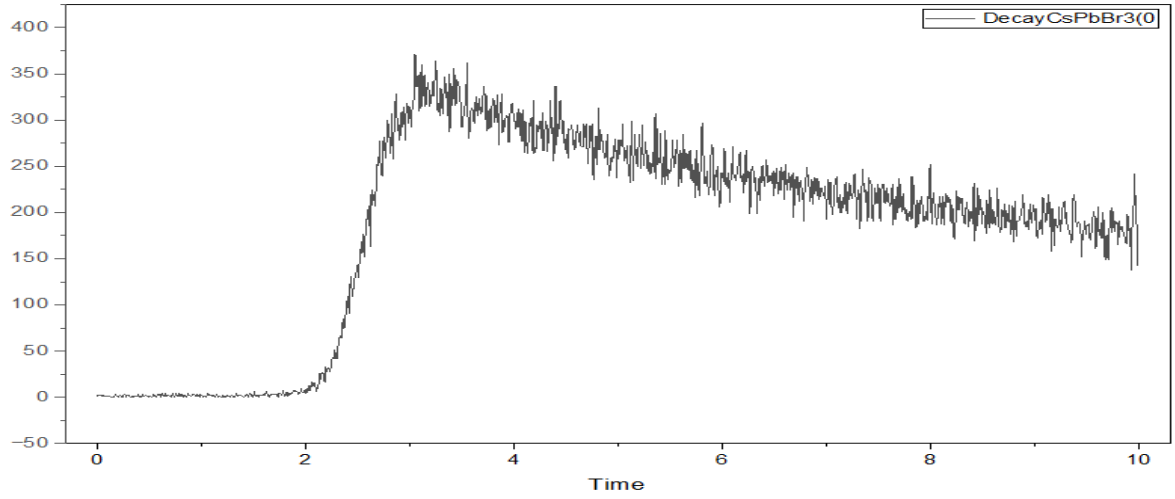
Online ISSN 3007-3197
Print ISSN 3007-3189

http://amresearchreview.com/index.php/Journal/about

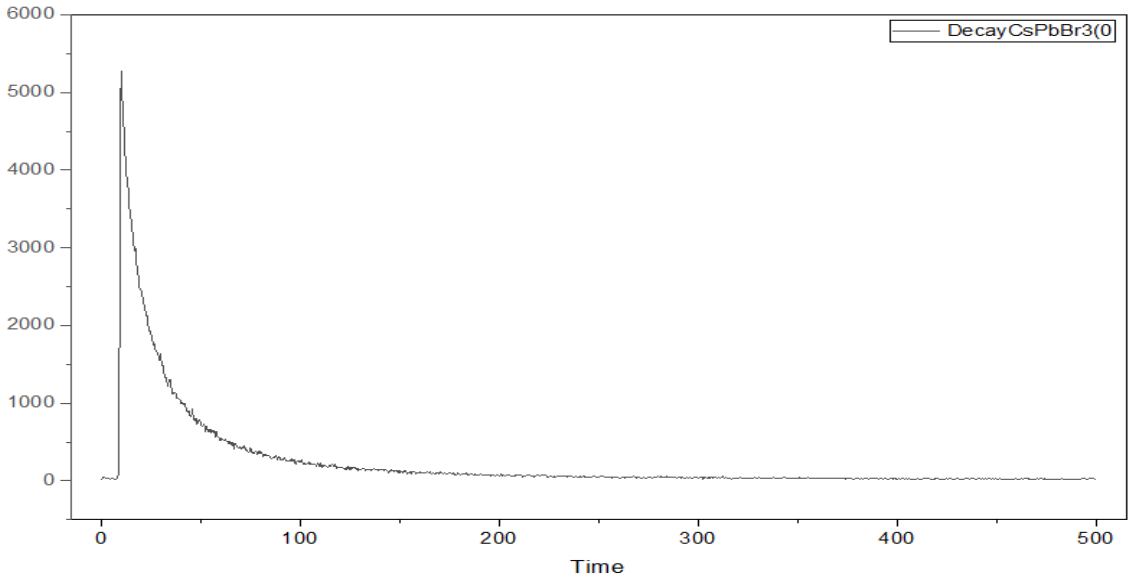
exchange on the material's photophysical properties.

Graph (a)Time-resolved photoluminescence (TRPL) decay profile of $CsPbBr_3$ nanocrystals.

The plot shows the temporal evolution of the photoluminescence (PL) intensity of $CsPbBr_3$ following photoexcitation. A sharp rise in PL intensity is observed within



the initial ~2 ns, corresponding to the fast exciton generation and radiative recombination processes. This is followed by a gradual decay extending up to 10 ns, indicating carrier relaxation and non-radiative recombination pathways. The relatively slow decay tail suggests trap-assisted recombination and surface-related defect states in the $CsPbBr_3$ nanocrystals. The overall decay dynamics provide crucial insights into exciton lifetimes, surface passivation quality, and the efficiency of radiative versus non-radiative processes in the material.



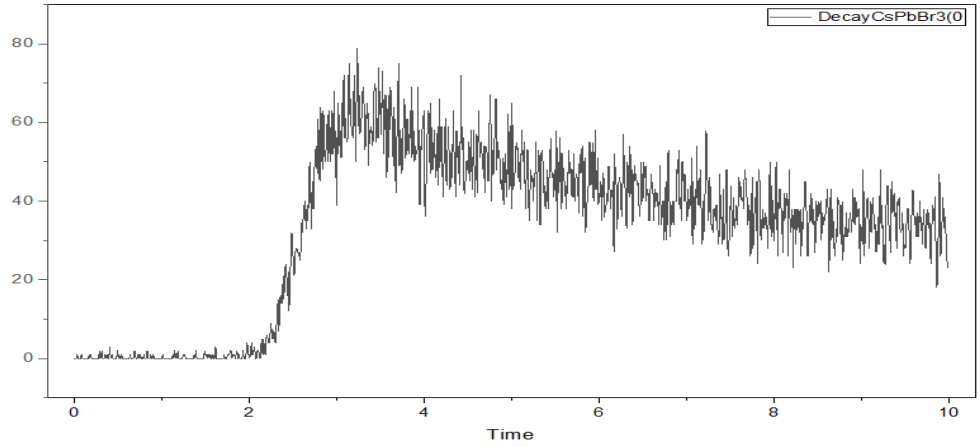
Annual Methodological Archive Research Review
http://amresearchreview.com/index.php/Journal/about
Volume 3, Issue 10 (2025)

Online ISSN 3007-3197
Print ISSN 3007-3189

http://amresearchreview.com/index.php/Journal/about

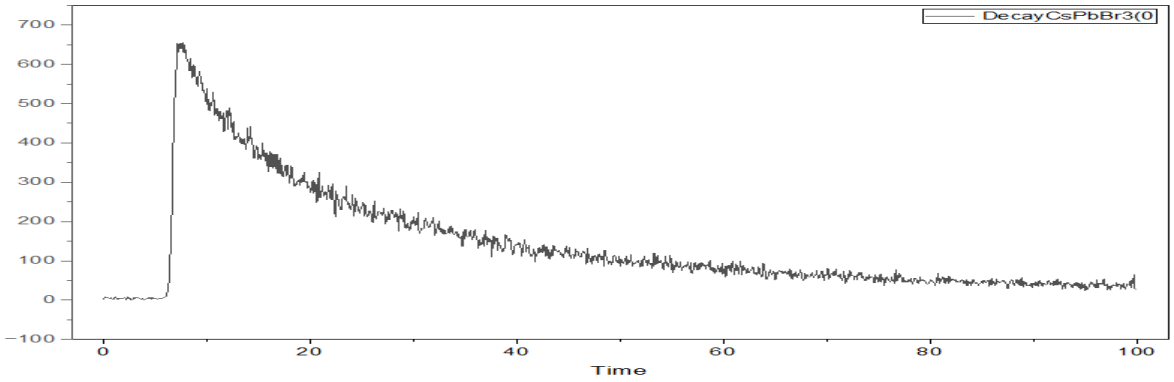
Graph (b)Photoluminescence (PL) decay dynamics of $CsPbBr_3$ nanocrystals over an extended time window.

The decay curve exhibits a sharp initial quenching within the first few nanoseconds, corresponding to rapid exciton recombination. This is followed by a long-lived tail that extends beyond 400 ns, indicating the presence of slower non-radiative recombination channels, such as trap-assisted processes or defect-state-mediated carrier relaxation. The pronounced biexponential-like behavior highlights the coexistence of fast radiative pathways and slower defect-related recombination, reflecting the intrinsic exciton dynamics and surface/interface quality of $CsPbBr_3$ nanocrystals.



Graph (c)Time-resolved photoluminescence (TRPL) profile of $CsPbBr_3$ nanocrystals.

The curve shows a rapid rise in emission intensity within the first ~2 ns, corresponding to exciton generation and radiative recombination. The subsequent decay is relatively shallow compared to Figure (a), with the PL intensity stabilizing at a higher baseline over the 10 ns window. This indicates suppressed non-radiative recombination and a stronger contribution from radiative pathways, suggesting improved surface passivation or reduced trap-state density in these nanocrystals. The overall dynamics reflect enhanced stability and prolonged exciton lifetimes relative to samples exhibiting faster quenching.



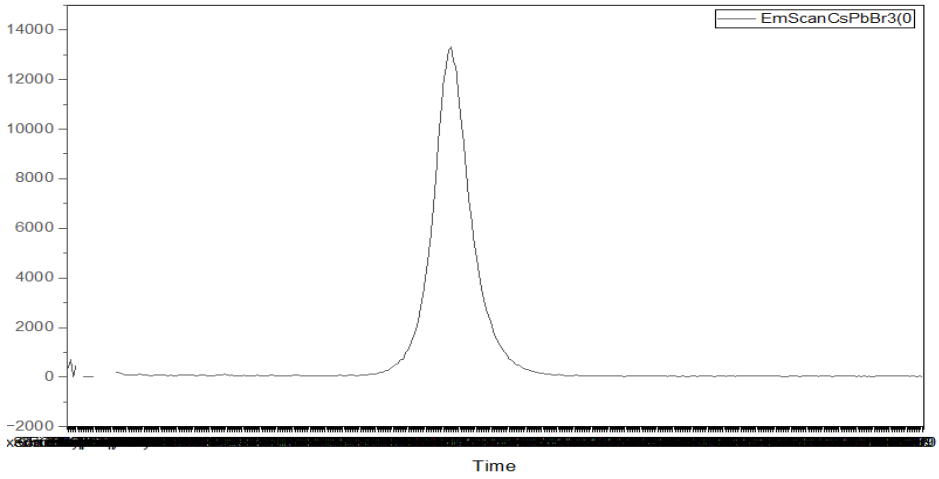
Graph (d)Photoluminescence (PL) decay dynamics of $CsPbBr_3$ nanocrystals over a 100 ns time window.

Annual Methodological Archive Research Review
http://amresearchreview.com/index.php/Journal/about
Volume 3, Issue 10 (2025)

Online ISSN 3007-3197
Print ISSN 3007-3189

http://amresearchreview.com/index.php/Journal/about

The decay profile exhibits a sharp rise in emission intensity within the first few nanoseconds, attributed to prompt exciton generation and radiative recombination. This is followed by a biexponential-like decay: a fast component (0–20 ns) linked to exciton recombination and surface-trap interactions, and a slower component extending up to ~100 ns, representing long-lived trap-mediated relaxation pathways. The persistence of the slower decay tail suggests the presence of defect states or surface imperfections that prolong carrier lifetimes. Such dynamics reveal the coexistence of efficient radiative processes with significant trap-assisted recombination, underscoring the importance of surface passivation in optimizing $CsPbBr_3$ nanocrystal performance.



Graph (e)Prompt emission scan of $CsPbBr_3$ nanocrystals.

The spectrum shows a sharp and symmetric emission peak with maximum intensity around ~13,000 counts, occurring within a narrow temporal window. The steep rise and fall indicate ultrafast exciton generation and recombination dynamics dominated by radiative processes. The absence of a pronounced long-lived tail suggests minimal trap-assisted recombination under these conditions. Such a profile is characteristic of highly crystalline $CsPbBr_3$ nanocrystals with efficient radiative pathways, reflecting their strong excitonic emission and high photoluminescence quantum yield (PLQY).

CONCLUSION

The present study demonstrates that surface modification of $CsPbBr_3$ nanocrystals with a newly synthesized chlorotriazine ligand significantly influences their photophysical properties. Tauc plot analysis revealed a modest but consistent blue shift in the optical band gap from 2.38 eV (control, OA/OAm-capped) to 2.40 eV (chlorotriazine-modified), accompanied by a sharper absorption onset and reduced Urbach energy, indicating diminished structural disorder and trap density. These findings were corroborated by derivative spectra and Urbach tail fitting, which confirmed improved band edge definition and lower energetic disorder in the ligand-functionalized samples. Time-resolved photoluminescence studies further established that chlorotriazine passivation suppresses non-radiative recombination, prolongs carrier lifetime, and enhances radiative emission efficiency. Collectively, these results

Online ISSN 3007-3197
Print ISSN 3007-3189
http://amresearchreview.com/index.php/Journal/about

confirm the working hypothesis that the electron-rich triazine ring and substitution pattern of the ligand enable strong coordination with surface Pb^{2+} and Br^- sites, thereby minimizing defect-assisted processes and stabilizing the nanocrystal surface. Although the observed band gap shift is small, the improvements in absorption sharpness, reduced sub-gap states, and extended photoluminescence lifetime demonstrate that ligand chemistry exerts a decisive role in tailoring optoelectronic quality. The enhanced optical stability and reduced recombination losses highlight the potential of chlorotriazine-functionalized $CsPbBr_3$ nanocrystals for high-performance optoelectronic devices such as light-emitting diodes, lasers, and photovoltaic cells.

REFERENCES

J. Liang et al., "Recent Progress and Development in Inorganic Halide Perovskite Quantum Dots for Photoelectrochemical Applications," Small, vol. 16, no. 15, p. 1903398, Apr. 2020, doi: 10.1002/smll.201903398.
Y. Wei, Z. Cheng, and J. Lin, "An overview on enhancing the stability of lead halide perovskite quantum dots and their applications in phosphor-converted LEDs," Chem. Soc. Rev., vol. 48, no. 1, pp. 310–350, 2019, doi: 10.1039/C8CS00740C.
J. Choi and B. H. Kim, "Ligands of Nanoparticles and Their Influence on the Morphologies of Nanoparticle-Based Films," Nanomaterials, vol. 14, no. 20, p. 1685, Oct. 2024, doi: 10.3390/nano14201685.
W. Wang et al., "Colloidal Inorganic Ligand-Capped Nanocrystals: Fundamentals, Status, and Insights into Advanced Functional Nanodevices," Chem. Rev., vol. 122, no. 3, pp. 4091–4162, Feb. 2022, doi: 10.1021/acs.chemrev.1c00478.
R. Diana and B. Panunzi, "The Role of Zinc(II) Ion in Fluorescence Tuning of Tridentate Pincers: A Review," Molecules, vol. 25, no. 21, p. 4984, Oct. 2020, doi: 10.3390/molecules25214984.
P. Reiss, M. Carrière, C. Lincheneau, L. Vaure, and S. Tamang, "Synthesis of Semiconductor Nanocrystals, Focusing on Nontoxic and Earth-Abundant Materials," Chem. Rev., vol. 116, no. 18, pp. 10731–10819, Sept. 2016, doi: 10.1021/acs.chemrev.6b00116.
N. Al-Shamsi, S. P. Laptenok, M. S. Bufaroosha, Y. E. Greish, and N. Saleh, "Time-resolved photoluminescence of 6-thienyl-lumazine fluorophores in cellulose acetate nanofibers for detection of mercury ions," Spectrochim. Acta. A. Mol. Biomol. Spectrosc., vol. 222, p. 117189, Nov. 2019, doi: 10.1016/j.saa.2019.117189.
S. Toso, D. Baranov, and L. Manna, "Metamorphoses of Cesium Lead Halide Nanocrystals," Acc. Chem. Res., vol. 54, no. 3, pp. 498–508, Feb. 2021, doi: 10.1021/acs.accounts.0c00710.
M. Abdi-Jalebi, M. Ibrahim Dar, A. Sadhanala, E. M. J. Johansson, and M. Pazoki, "Optical absorption and photoluminescence spectroscopy," in Characterization Techniques for Perovskite Solar Cell Materials, Elsevier, 2020, pp. 49–79. doi: 10.1016/B978-0-12-814727-6.00003-7.
A. Sethiya, D. K. Jangid, J. Pradhan, and S. Agarwal, "Role of cyanuric chloride in organic synthesis: A concise overview," J. Heterocycl. Chem., vol. 60, no. 9, pp. 1495–1516, Sept. 2023, doi: 10.1002/jhet.4661.
A. Jordan, P. Stoy, and H. F. Sneddon, "Chlorinated Solvents: Their Advantages, Disadvantages, and Alternatives in Organic and Medicinal Chemistry," Chem. Rev.,

Online ISSN 3007-3197
Print ISSN 3007-3189

vol. 121, no. 3, pp. 1582–1622, Feb. 2021, doi: 10.1021/acs.chemrev.0c00709.
Y. Shen, M. Y. Gee, and A. B. Greytak, "Purification technologies for colloidal nanocrystals," Chem. Commun., vol. 53, no. 5, pp. 827–841, 2017, doi: 10.1039/C6CC07998A.
M. M. Krause and P. Kambhampati, "Linking surface chemistry to optical properties of semiconductor nanocrystals," Phys. Chem. Chem. Phys., vol. 17, no. 29, pp. 18882–18894, 2015, doi: 10.1039/C5CP02173A.
S. Daniel, "Characterization of carbon dots," in Carbon Dots in Analytical Chemistry, Elsevier, 2023, pp. 43–58. doi: 10.1016/B978-0-323-98350-1.00015-3.
Md. F. Rahman, J. Hossain, and A. B. Md. Ismail, "Structural, surface morphological and optical properties and their correlation with the thickness of spin coated superior quality CdS thin film synthesized using a novel chemical route," SN Appl. Sci., vol. 2, no. 12, p. 1956, Dec. 2020, doi: 10.1007/s42452-020-03836-2.
V. R. Akshay, B. Arun, G. Mandal, and M. Vasundhara, "Visible range optical absorption, Urbach energy estimation and paramagnetic response in Cr-doped TiO_2 nanocrystals derived by a sol–gel method," Phys. Chem. Chem. Phys., vol. 21, no. 24, pp. 12991–13004, 2019, doi: 10.1039/C9CP01351B.
J. Hou, H.-Y. Chen, S. Zhang, G. Li, and Y. Yang, "Synthesis, Characterization, and Photovoltaic Properties of a Low Band Gap Polymer Based on Silole-Containing Polythiophenes and 2,1,3-Benzothiadiazole," J. Am. Chem. Soc., vol. 130, no. 48, pp. 16144–16145, Dec. 2008, doi: 10.1021/ja806687u.
S. Akhil, V. G. V. Dutt, R. Singh, and N. Mishra, "Surface-State-Mediated Interfacial Hole Transfer Dynamics between $CsPbBr_3$ Perovskite Nanocrystals and Phenothiazine Redox Couple," J. Phys. Chem. C, vol. 125, no. 40, pp. 22133–22141, Oct. 2021, doi: 10.1021/acs.jpcc.1c07129.
Y. Sun, J. Zhang, H. Yu, C. Huang, and J. Huang, "Several Triazine-Based Small Molecules Assisted in the Preparation of High-Performance and Stable Perovskite Solar Cells by Trap Passivation and Heterojunction Engineering," ACS Appl. Mater. Interfaces, vol. 14, no. 5, pp. 6625–6637, Feb. 2022, doi: 10.1021/acsami.1c21081.
B. G. Alberding, A. J. Biacchi, A. R. Hight Walker, and E. J. Heilweil, "Charge Carrier Dynamics and Mobility Determined by Time-Resolved Terahertz Spectroscopy on Films of Nano-to-Micrometer-Sized Colloidal Tin(II) Monosulfide," J. Phys. Chem. C, vol. 120, no. 28, pp. 15395–15406, July 2016, doi: 10.1021/acs.jpcc.6b01684.
D. He, F. Zhao, C. Wang, and Y. Lin, "Non-Radiative Recombination Energy Losses in Non-Fullerene Organic Solar Cells," Adv. Funct. Mater., vol. 32, no. 19, p. 2111855, May 2022, doi: 10.1002/adfm.202111855.
M. Q. Zakariaet al., "Ultrafast Laser Irradiation Enhances Crystallinity and Photoluminescence of Colloidal $CsPbBr_3$ Nanocrystals for High-Performance X-ray Detection," ACS Appl. Nano Mater., vol. 8, no. 34, pp. 16985–16993, Aug. 2025, doi: 10.1021/acsanm.5c03636.
J. Chen, J. Lv, X. Liu, J. Lin, and X. Chen, "A study on theoretical models for investigating time-resolved photoluminescence in halide perovskites," Phys. Chem. Chem. Phys., vol. 25, no. 11, pp. 7574–7588, 2023, doi: 10.1039/D2CP05723A.